small counterions have been elucidated. Magnetic-susceptibility measurements on $Co_{0.37}Na_{0.14}Pt_3O_4$ (Schwartz & Parise, 1982) yield evidence that the cobalt present is in the divalent state and is consistent with the model suggested of multiple site occupancy for cobalt.

The details of the $Ni_xPt_3O_4$ structure are still problematic. Ordering reflections in both $Ni_{0.25}Pt_3O_4$ and $Ni_xNa_yPt_3O_4$ suggest a situation similar to that described above for $Co_{0.37}Na_{0.14}Pt_3O_4$. The poor quality of diffraction data collected suggests $Ni_{0.25}Pt_3O_4$ and $Ni_xNa_yPt_3O_4$ are poorly crystallized compounds. This may be related to the extremely small size of Ni relative to other cations found in the $M_xPt_3O_4$ structural family. These compositions remain an outstanding problem within the $M_xPt_3O_4$ series.

We would like to thank D. E. Cox for his most generous and invaluable contributions of time, effort and expertise throughout this entire project, C. M. Foris for assistance with the Guinier photographs, B. F. Burgess and C. R. Perrotto for atomic absorption analyses. L. M. Corliss and J. M. Hastings of Brookhaven National Laboratory collected neutron powder diffraction data at $\lambda = 1{\cdot}343$ Å for all samples. The work was performed under NSF Grant DMR79-06900 and at the Experimental Station of E.I. du Pont de Nemours and Company.

References

BACON, G. E. (1978). Brookhaven National Laboratory compilation (unpublished).
BERGMAN, J. G. & COTTON, F. A. (1966). *Inorg. Chem.* **5**, 1208–1213.
BERGNER, V. D. & KOHLHAAS, R. (1973). *Z. Anorg. Allg. Chem.* **401**, 15–20.
BURDETT, J. K., HOFFMANN, R. & FAY, R. C. (1978). *Inorg. Chem.* **17**, 2553–2568.
BURNS, R. G. (1971). In *Mineralogical Applications of Crystal Field Theory*. Cambridge Univ. Press.
CAHEN, D., IBERS, J. A. & MUELLER, M. H. (1974). *Inorg. Chem.* **13**, 110–115.
CAHEN, D., IBERS, J. A. & SHANNON, R. D. (1972). *Inorg. Chem.* **11**, 2311–2315.
CAHEN, D., IBERS, J. A. & WAGNER, J. B. (1974). *Inorg. Chem.* **13**, 1377–1388.
HEWAT, A. E. (1973). UK Atomic Energy Authority Research Group Report RLL 73/897 (unpublished).
HEWAT, A. E. (1979). *Acta Cryst.* A**35**, 248.
HOARD, J. L. & SILVERTON, J. V. (1963). *Inorg. Chem.* **2**, 235–243.
JOHNSON, C. K. (1965). *ORTEP*. Report ORNL-3794. Oak Ridge National Laboratory, Tennessee.
KEPERT, D. L. (1965). *J. Chem. Soc.* pp. 4736–4744.
KOESTER, L. (1977). *Springer Tracts Mod. Phys.* **80**, 1–55.
LAZAREV, V. B. & SHAPLYGIN, I. S. (1978*a*). *Russ. J. Inorg. Chem.* **23**, 163–170.
LAZAREV, V. B. & SHAPLYGIN, I. S. (1978*b*). *Russ. J. Inorg. Chem.* **23**, 1610–1612.
LAZAREV, V. B. & SHAPLYGIN, I. S. (1978*c*). *Mater. Res. Bull.* **13**, 229–235.
RIETVELD, H. M. (1969*a*). Reactor Centrum Nederland Research Report RCN 104 (unpublished).
RIETVELD, H. M. (1969*b*). *J. Appl. Cryst.* **2**, 65–71.
SCHWARTZ, K. B. & PARISE, J. B. (1982). *J. Phys. Chem. Solids*. In the press.
SCHWARTZ, K. B., PREWITT, C. T., SHANNON, R. D., CORLISS, L. M., HASTINGS, J. M. & CHAMBERLAND, B. L. (1982). *Acta Cryst.* B**38**, 363–368.
SHANNON, R. D. (1976). *Acta Cryst.* A**32**, 751–767.
SHANNON, R. D., GIER, T. E., CARCIA, P. F., BIERSTEDT, P. E., FLIPPEN, R. B. & VEGA, A. J. (1982). *Inorg. Chem.* In the press.
WASER, J. & MCCLANAHAN, E. D. (1951). *J. Chem. Phys.* **19**, 413–416.
WILL, G. (1979). *J. Appl. Cryst.* **12**, 483–485.

Acta Cryst. (1982). B**38**, 2116–2120

Deformation Density in Complex Anions. III.* Potassium Perchlorate

BY J. W. BATS AND H. FUESS

Institut für Kristallographie und Mineralogie der Universität Frankfurt, Senckenberganlage 30, *Postfach* 11 19 32, 6000 *Frankfurt am Main* 11, *Federal Republic of Germany*

(*Received* 1 *December* 1981; *accepted* 3 *March* 1982)

Abstract

$KClO_4$, space group *Pnma*, $Z = 4$, $a = 8{\cdot}765$ (1), $b = 5{\cdot}620$ (1), $c = 7{\cdot}205$ (1) Å, $V = 354{\cdot}9$ (1) Å^3 at 120 K. Neutron diffraction: ω scan, $\lambda = 1{\cdot}0272$ (5) Å, 831 independent reflections, $(\sin\theta/\lambda)_{max} = 0{\cdot}80$ Å^{-1}, $R_w(F) = 0{\cdot}022$. X-ray diffraction: ω–2θ scan, Mo $K\alpha$ radiation, two crystals: (I) 1884 reflections, $(\sin\theta/\lambda)_{max} = 1{\cdot}08$ Å^{-1}, $R_w(F) = 0{\cdot}030$; (II) 1153 reflections,

* Part II: Fuess, Bats, Dannöhl, Meyer & Schweig (1982).

0567-7408/82/082116-05$01.00

$(\sin\theta/\lambda)_{max} = 0.90$ Å^{-1}, $R_w(F) = 0.028$. The deformation density has been determined by the X–N technique. The noise level of the X–N density has been reduced by a multipole expansion of the deformation density. Peaks of about 0.35 e Å^{-3} are found in all the Cl–O bonds. Lone-pair density with peak heights ranging from 0.1 to 0.4 e Å^{-3} is found at all the O atoms under angles of 95–100° with the Cl–O bonds.

Introduction

Our interest lies in the study of the deformation electron density in complexes containing the second-row elements such as silicates, sulfates and chlorates. In the present paper we present our results on $KClO_4$.

The crystal structure of $KClO_4$ was determined by Gottfried & Schusterius (1933) and refined by Mani (1957) and Johansson & Lindqvist (1977). The present work is based on a combined X-ray and neutron diffraction study at 120 K.

Experimental

Suitable crystals were obtained by recrystallization of $KClO_4$ from an aqueous solution. The cell constants were determined in the X-ray experiment from the setting angles of 15 reflections. A review of the diffraction experiments is given in Tables 1 and 2.*

Neutron diffraction

The four-circle $P32$ diffractometer at the Kernforschungszentrum Karlsruhe was used: crystal dimensions 2.3 × 2.2 × 2.0 mm; Air Products Displex cryostat, temperature 120 (±1) K; ω-scan mode; two to four equivalent reflections; profile analysis; two standard reflections after every 50 reflections, long-range fluctuations of 2.5%, data rescaling with respect to the standards; absorption correction; weights $w(I) = [\sigma^2(I)_{counting} + (0.03I)^2]^{-1}$. The weight of an averaged reflection was equal to the sum of the weights of the individual reflections.

X-ray diffraction

A Syntex $P2_1$ diffractometer with Nb-filtered Mo $K\alpha$ radiation was used: $\omega/2\theta$ scan; temperature 120 K, Enraf–Nonius low-temperature device, thermocouple in the cold-air stream, calibrated by studying the phase transition of KH_2PO_4 at 122.8 K; two sets of X-ray data from two crystals; two to seven equivalent reflections; profile analysis (Blessing, Coppens & Becker, 1974).

Three standard reflections were remeasured after every 60 reflections: maximum fluctuations of 3%, no intensity decrease due to radiation decay, data were rescaled with respect to the standards; absorption correction was by numerical integration over 8 × 8 × 8 Gaussian grid points. The equivalent reflections were averaged. The weighting scheme was the same as for neutrons.

Structure refinement

Neutron diffraction

Scattering lengths for Cl and O were taken from Koester (1977). The scattering length of K, which is less well known, was refined together with the structural parameters. The value obtained, $b_K = 3.65$ (2) fm, is slightly smaller than the value of 3.71 (2) fm reported by Koester (1977).

* See deposition footnote.

Table 1. *Review of least-squares refinements*

	Number of reflections	Number of parameters	Scale factor	$R(F)$	$R_w(F)$	S*
Neutron						
Conventional refinement	831	41	–	0.055	0.022	1.02
X-ray crystal 1						
All-data refinement	1884	35	2.552 (4)	0.042	0.030	2.23
$\sin\theta/\lambda > 0.75$ Å^{-1}	1219	34	2.528 (12)	0.065	0.034	1.28
Multipole refinement (positional and thermal parameters of Cl and O fixed)	1887	112	2.556 (3)	0.038	0.020	1.47
X-ray crystal 2						
All-data refinement	1153	35	2.604 (6)	0.026	0.028	2.31
$\sin\theta/\lambda > 0.75$ Å^{-1}	484	33	2.559 (14)	0.034	0.025	1.36
Multipole refinement (positional and thermal parameters of Cl and O fixed)	1156	112	2.591 (4)	0.022	0.018	1.51

* $S = [\sum w(F_o - |F_c|)^2/(n_o - n_v)]^{1/2}$.

Table 3. *Positional parameters and equivalent values of the anisotropic thermal parameters from the neutron diffraction data*

$U_{eq} = \frac{1}{3}$ trace **U**.

	x	y	z	U_{eq} (Å^2)
K	0·18038 (14)	0·25	0·33865 (16)	0·0120 (5)
Cl	0·06954 (5)	0·25	0·81160 (6)	0·00870 (17)
O(1)	0·19372 (10)	0·25	0·94289 (10)	0·0150 (4)
O(2)	0·08098 (7)	0·04086 (8)	0·69491 (8)	0·0138 (2)
O(3)	−0·07410 (11)	0·25	0·90607 (12)	0·0185 (4)

An extinction correction was made using the formalism of Coppens & Hamilton (1970). A type I anisotropic extinction correction was found to give slightly better agreement factors than type II anisotropic or isotropic extinction. The minimum transmission factor for extinction was $y = F^2_{obs}/F^2_{corr} = 0{\cdot}703$ for the 040 reflection. No atomic parameters changed more than $\frac{1}{2}\sigma$ among the different types of extinction refinement, while the scale factor was unaffected by the type of extinction treatment.

An attempt to include third-cumulant thermal coefficients (Johnson, 1970) did not lead to any significant improvement. Final agreement factors are reported in Table 1, atomic parameters in Table 3.*

X-ray diffraction

Scattering factors were taken from *International Tables for X-ray Crystallography* (1974). Anomalous-dispersion factors (Cromer & Liberman, 1970) were applied to all atoms. An isotropic extinction coefficient was refined as described by Larson (1969). For each of the two data sets two kinds of refinement were performed: (i) a conventional refinement using all the data and (ii) a high-angle refinement using only those reflections with $\sin\theta/\lambda > 0{\cdot}75$ Å^{-1}. In the latter refinement the extinction coefficient was kept invariant. In data set 2 the scale factor showed a considerable correlation with the thermal parameters in the high-angle range. Consequently it was fixed at a value obtained by a refinement on the data with $\sin\theta/\lambda > 0{\cdot}65$ Å^{-1}.

Agreement factors, positional parameters and the anisotropic thermal parameters are reported in Tables 1 and 4.*

* Lists of structure factors, Fig. 1(*b*) (*X*–*X* density), Table 2 (a summary of the data collection), Table 4 (positional and anisotropic thermal parameters for all data sets) and Table 6 (systematic differences in thermal parameters) have been deposited with the British Library Lending Division as Supplementary Publication No. SUP 36812 (35 pp.). Copies may be obtained through The Executive Secretary, International Union of Crystallography, 5 Abbey Square, Chester CH1 2HU, England.

Discussion

Bond distances and angles derived from the neutron data set are reported in Table 5. The structure at 120 K is similar to the room-temperature structure (Johansson & Lindqvist, 1977).

All positional parameters derived from the neutron and the two X-ray data sets are very similar (Table 4). In order to detect any significant differences, the various sets were analyzed with the help of half-normal probability plots (Hamilton & Abrahams, 1972). The only differences ($2{\cdot}5$ and $3{\cdot}0\sigma$) larger than the expected values ($1{\cdot}9\sigma$) occur for atom O(3), when X-ray data set 1 is compared with the neutron results. These differences are found in both the refinement on all the X-ray reflections and in the high-angle refinement, although the shifts are in different directions. The positional parameters derived from X-ray data set 2 do not differ significantly from the neutron diffraction results.

Larger differences are found, however, when the temperature factors of the various parameter sets are compared. Systematic differences along the unit-cell axes, averaged over the five atoms, are given in Table 6.*

Obviously the neutron determination gives larger values for U_{11} and U_{22} and smaller values for U_{33} than the two X-ray determinations [largest difference, $\Delta U_{22} = 0{\cdot}00087\ (15)$ Å^2]. The X-ray results are more consistent, although a difference of 3σ is found in U_{11} [$\Delta U_{11} = 0{\cdot}00030\ (9)$ Å^2]. Similar discrepancies in thermal parameters are often found in combined X-ray and neutron diffraction studies (Fuess, Bats, Dannöhl, Meyer & Schweig, 1982) and are believed to result from an accumulation of systematic effects like errors in the absorption and extinction correction, instrumental misalignments, truncation errors at large diffraction angles (Denne, 1977) and the neglect of thermal and structural diffuse scattering. These inconsistencies in thermal parameters have to be taken into account

* See deposition footnote.

Table 5. *Bond distances* (Å) *and angles* (°) *based on the neutron diffraction results*

Values in square brackets have been corrected for libration.

Cl–O(1)	1·4418 (10) [1·449 (1)]	2 × K–O(2)	2·8245 (12)
		K–O(3)	2·8309 (16)
2 × Cl–O(2)	1·4485 (6) [1·456 (1)]	2 × K–O(2)	2·8497 (12)
		K–O(1)	2·8542 (14)
Cl–O(3)	1·4316 (10) [1·440 (1)]	2 × K–O(2)	2·9544 (13)
		2 × K–O(1)	3·1110 (7)
		2 × K–O(3)	3·4454 (9)
O(1)–Cl–O(2)	109·17 (4)	O(2)–Cl–O(2)	108·46 (4)
O(1)–Cl–O(3)	110·62 (6)	O(2)–Cl–O(3)	109·69 (4)

before the calculation of electron density maps with the *X–N* technique can be performed. The electron density distribution in $KClO_4$ has been analyzed in a number of different ways.

(I) A difference Fourier synthesis has been calculated using the reflections with $\sin\theta/\lambda \leq 0{\cdot}80$ Å^{-1} and the atomic parameters from the high-angle refinements. The corresponding *X–X* (high-angle) density is shown in Fig. 1(*b*)* in the O(2)–Cl–O(3) section for both the X-ray data sets. The two maps agree within 0·1 e Å^{-3}.

(II) *X–N* electron densities have been calculated for both the X-ray data sets. To account for the systematic differences in thermal parameters among the X-ray and neutron thermal parameters, the neutron thermal parameters have been modified by adding the correction factors reported in Table 6. The resulting *X–N* densities were again rather similar for the two data sets. Subsequently the two *X–N* densities were averaged. This was achieved by a weighted averaging of the Fourier coefficients of the two data sets. The corresponding average *X–N* density has been calculated up to $\sin\theta/\lambda = 0{\cdot}85$ Å^{-1} and is shown in the left-hand side of Fig. 1(*a*) for a number of O–Cl–O sections.

* See deposition footnote.

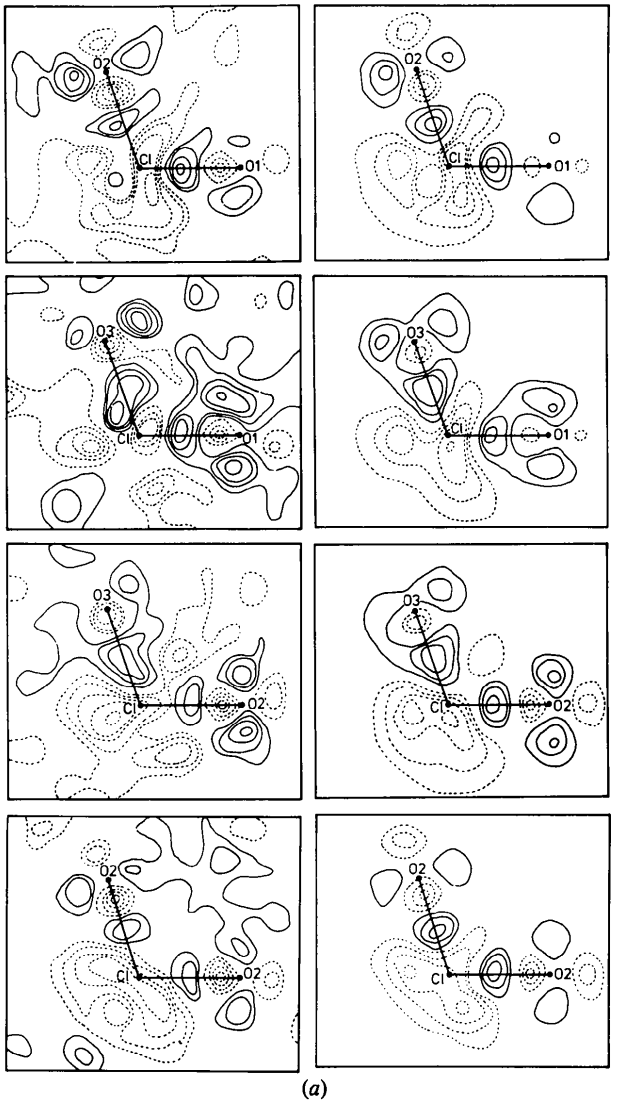

(*a*)

Fig. 1. (*a*) *X–N* deformation density in a number of O–Cl–O sections, averaged over the two data sets. Contour interval 0·1 e Å^{-3}, negative contours dashed, zero contour omitted. At left: the normal *X–N* density; at right: a multipole expansion of the *X–N* density.

A measure of the accuracy of the electron density is the statistical error averaged over the unit cell $\sigma(\bar{\rho}) = (2\sqrt{2}/V)[\sum\sigma^2(F)]^{1/2}$ (Cruickshank, 1949) and is 0·047 e Å^{-3} for the present result. This value explains the spurious peaks, *i.e.* peaks or troughs at places where no density is expected, of about 0·15 e Å^{-3} ($= 3\sigma$) in the general position and 0·20 e Å^{-3} in the mirror plane where errors tend to accumulate.

In order to reduce the noisy appearance of the electron density distribution it has been attempted to filter the data using a multipole-expansion method.

(III) The multipole-expansion formalism *LSEXP* (Hirshfeld, 1977) has been applied to both X-ray data sets. A full set of multipole coefficients (monopole up to hexadecapole) was assigned to Cl and each of the three independent O atoms. The exponents of the radial dependent functions $\exp(-\alpha r)$ were fixed to $\alpha = 6{\cdot}0$. The K atom was supposed to be ionic. It was assigned a K^+ scattering factor and no deformation functions. The structure was constrained to be neutral. In initial trials the positional and thermal parameters of the atoms were refined simultaneously with the deformation coefficients and the scale factor. However, the temperature factors and scale factor were correlated with the monopole coefficients and the positional parameters with the dipole terms. Some of the resulting positional parameters were significantly different from the neutron values resulting in a highly artificial electron density distribution. Therefore, we kept the positional and thermal parameters of the Cl and O atoms fixed to the neutron values. The thermal parameters were again modified as described above. The *R* factors resulting from these multipole refinements have been included in Table 1. They are much lower than those of the conventional X-ray refinements. Residual densities were calculated following these refinements. Residual peaks up to 0·15 e Å^{-3} were found. None was significant, however, with respect to the statistical error in the Fourier syntheses. The multipole coefficients obtained from the two data sets were averaged and used to calculate a dynamic deformation density up to a resolution of $\sin\theta/\lambda = 0{\cdot}90$ Å^{-1}. Corresponding sections are shown in the right-hand side of Fig. 1(*a*) for comparison with the *X–N* density. Similar sections based on the static deformation density showed higher peaks. In contrast

to the dynamic density, however, the static density appeared to be rather sensitive to the choice of the radial exponents α. The quality of the data is probably not sufficient to deduce the static density. The dynamic density appears less dependent. Consequently we prefer to base our discussion on the dynamic instead of the static deformation density.

The dynamic density is very similar to the *X–N* density. This is not surprising as fixing of the positional and thermal parameters would require this result. The main advantage of the multipole deformation density is that the spurious peaks have disappeared, resulting in a smooth electron density with peaks better centered in the bonds.

The three independent Cl–O bonds show a good similarity. Excess electron density is observed at the midpoints of the Cl–O bonds with a peak height of about 0·35 e Å^{-3}. Lone-pair peaks are found at the O atoms under angles of 95° to 100°. Troughs are found near the O atoms in the Cl–O bonds. The vicinity of the Cl atom is electron deficient and shows minima in the extension of the O–Cl bonds.

Comparison of Figs. 1(*a*) and 1(*b*) shows that the *X–N* and *X–X* (high-angle) maps give a rather similar density in the Cl–O bonds. The lone-pair density at the O atoms, however, is not well reproduced in the *X–X* density. This indicates a contribution of the deformation electron density to the X-ray reflections at higher angles.

The deformation density in $KClO_4$ shows little resemblance to the multipole deformation densities of NH_4ClO_4 and $NaClO_4.H_2O$ reported by Lundgren (1979, 1980). That author, however, reported a high correlation between multipole coefficients and structural parameters. Therefore, it is doubtful whether these multipole densities correspond to the actual deformation electron density in these compounds.

Fig. 2 shows the dynamic deformation density in cross sections through the midpoints of the Cl–O bonds. The electron density has an approximate cylinder symmetry about the bond. Cross sections through the O atoms perpendicular to the Cl–O bonds are given in Fig. 3 and show the distribution of the lone-pair peaks about the O atoms. The lone-pair density has a circular shape about the O atoms but with two maxima at opposite sides of each O atom. The

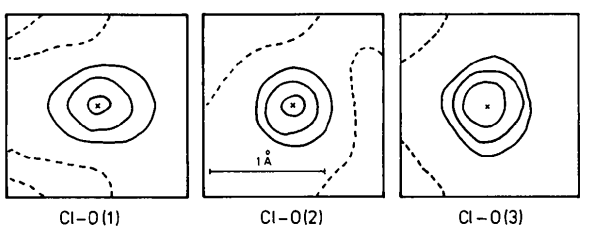

Fig. 2. Multipole *X–N* density in cross sections through the midpoints of the Cl–O bonds. Contours as in Fig. 1.

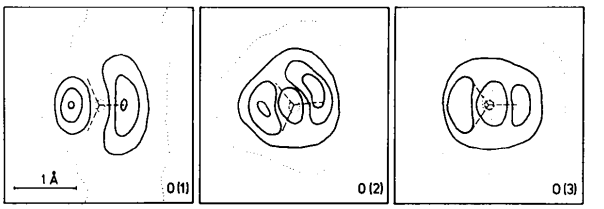

Fig. 3. Multipole *X–N* density in cross sections through the O atoms perpendicular to the Cl–O bonds. Contour interval 0·1 e Å^{-3}, negative contours dashed, zero contour dotted.

same features were found in the unfiltered *X–N* densities. The direction of the K···O interactions is given in the figures, but there appears no clear correlation between the positions of the maxima and the K···O bonds. The positions of the lone-pair peaks correspond to the p_π orbitals of unhybridized O atoms. It appears, however, that the lone-pair density is not evenly distributed over both p_π orbitals. The deformation density near K was featureless, if the errors of the map were taken into account.

We wish to thank Mr Massing and Dr P. Schweiss for technical assistance with the neutron diffraction experiment. Work was supported by the Deutsche Forschungsgemeinschaft and the Bundesministerium für Forschung und Technologie.

References

BLESSING, R. H., COPPENS, P. & BECKER, P. (1974). *J. Appl. Cryst.* **7**, 488–492.

COPPENS, P. & HAMILTON, W. C. (1970). *Acta Cryst.* A**26**, 71–83.

CROMER, D. T. & LIBERMAN, D. (1970). *J. Chem. Phys.* **53**, 1891–1898.

CRUICKSHANK, D. W. J. (1949). *Acta Cryst.* **2**, 65–82.

DENNE, W. A. (1977). *Acta Cryst.* A**33**, 438–440.

FUESS, H., BATS, J. W., DANNÖHL, H., MEYER, H. & SCHWEIG, A. (1982). *Acta Cryst.* B**38**, 736–743.

GOTTFRIED, C. & SCHUSTERIUS, C. (1933). *Z. Kristallogr.* **84**, 65–73.

HAMILTON, W. C. & ABRAHAMS, S. C. (1972). *Acta Cryst.* A**28**, 215–218.

HIRSHFELD, F. L. (1977). *Isr. J. Chem.* **16**, 226–229.

International Tables for X-ray Crystallography (1974). Vol. IV. Birmingham: Kynoch Press.

JOHANSSON, G. B. & LINDQVIST, O. (1977). *Acta Cryst.* B**33**, 2918–2919.

JOHNSON, C. K. (1970). *Thermal Neutron Diffraction*, edited by B. T. M. WILLIS, pp. 132–160. Oxford Univ. Press.

KOESTER, L. (1977). *Springer Tracts in Modern Physics.* Vol. 80. *Neutron Physics*, edited by G. HÖHLER. Berlin: Springer-Verlag.

LARSON, A. C. (1969). *Crystallographic Computing*, edited by F. R. AHMED, pp. 291–294. Copenhagen: Munksgaard.

LUNDGREN, J.-O. (1979). *Acta Cryst.* B**35**, 1027–1033.

LUNDGREN, J.-O. (1980). *Acta Cryst.* B**36**, 1774–1781.

MANI, N. V. (1957). *Proc. Indian Acad. Sci. Sect. A*, **46**, 143–151.